Please cite as: **Wu JC, Hutchings CH, Lindsay MJ, Werner CJ, Bundy BC. 2014. Enhanced Enzyme Stability Through Site-Directed Covalent Immobilization. Journal of Biotechnology. 193(1):83-90.**

Enhanced Enzyme Stability Through Site-Directed Covalent Immobilization

Jeffrey Chun Yu Wu, Christopher Hayden Hutchings, Mark Jeffrey Lindsay,
Christopher James Werner, Bradley Charles Bundy*
Department of Chemical Engineering, Brigham Young University, Provo, Utah

* Corresponding Author
Bradley C. Bundy
Department of Chemical Engineering
Brigham Young University
350S Clyde Building
Provo, Utah 84602
United States of America
Tel: +001 801-422-2807
Email: bundy@byu.edu

Keywords
- biocatalysis
- enzyme immobilization
- enzyme stability
- unnatural amino acids
- green manufacturing
- cell-free protein synthesis

Abstract Word Count: 170
Manuscript Word Count (excluding references): 3663

Abstract

Breakthroughs in enzyme immobilization have enabled increased enzyme recovery and reusability, leading to significant decreases in the cost of enzyme use and fueling biocatalysis growth. However, current enzyme immobilization techniques suffer from leaching, enzyme stability, and recoverability and reusability issues. Moreover, these techniques lack the ability to control the orientation of the immobilized enzymes. To determine the impact of orientation on covalently immobilized enzyme activity and stability, we apply our PRECISE (Protein Residue-Explicit Covalent Immobilization for Stability Enhancement) system to a model enzyme, T4 lysozyme. The PRECISE system uses non-canonical amino acid incorporation and the Huisgen 1,3-dipolar cycloaddition "click" reaction to enable directed enzyme immobilization at rationally chosen residues throughout an enzyme. Unlike previous site-specific systems, the PRECISE system is a truly covalent immobilization method. Utilizing this system, enzymes immobilized at proximate and distant locations from the active site were tested for activity and stability under denaturing conditions. Our results demonstrate that orientation control of covalently immobilized enzymes can provide activity and stability benefits exceeding that of traditional random covalent immobilization techniques. PRECISE immobilized enzymes were 50% and 73% more active than randomly immobilized enzymes after harsh freeze-thaw and chemical denaturant treatments.

1. Introduction

According to Environmental Protection Agency statistics, the U.S. alone contains more than 13,500 chemical manufacturing facilities providing shipments valued at over $555 billion annually (EPA, 2011). Unfortunately, traditional chemical manufacturing processes often require the use of toxic reagents, strong acids and bases, and have high energy costs while suffering from low product specificity. These processes produce more than 1.5 million tons of air pollution and over 10 billion pounds of solid waste annually, much of it toxic (EPA, 2011).

A more environmentally friendly alternative to conventional processes is the use of biocatalysts, or enzymes, to catalyze reactions (Bornscheuer et al., 2012). Enzyme use eliminates the need for many toxic reagents, enables reactions to be performed in aqueous conditions at ambient temperatures, and reduces the need for purification while providing high chemo-, regio-, enantio-, and stereo-specificity (Sheldon, 2007). These advantages have fueled a 7.5% annual growth rate in the industrial enzyme biocatalysis market from 1995 to 2012 (240% total increase in market share) such that enzyme biocatalysis represented 10% of the global catalysis market in 2012 (Kirk et al., 2002; Milmo, 2012) However, enzymes have their own unique set of challenges including the following: enzyme production costs, enzyme stability, and enzyme recoverability and reusability (Wang et al., 2009).

Enzyme immobilization provides a simple and elegant solution to these challenges. It enables recovery and reuse of the biocatalysts, significantly driving down the biocatalyst cost over many reactions. Currently, a number of different enzyme immobilization techniques are being used in industry such as enzyme adsorption, entrapment, and cross-linking (Sheldon, 2007). A particularly attractive method is attachment/adsorption of the enzyme to the surface of a carrier which commonly results in enhanced enzyme stability (Alonso et al., 2005; Anwar et al., 2007;

López-Gallego et al., 2005; Mozhaev et al., 1990; Qiu et al., 2005; Rocchietti et al., 2004). Stability enhancements have been shown after attachment to many different carriers, examples include including magnetic beads (Qiu et al., 2005), mesoporous sol-gel glass (Wang et al., 2001), silica nanospheres (Wang and Caruso, 2004), Sepabeads (Rocchietti et al., 2004), agarose (Rocchietti et al., 2004), and protein-coated microcrystals (Kreiner and Parker, 2005). Many different conjugation chemistries have been used, relying on amine, epoxy, maleic anhydride, glyoxal, biotin/streptavidin, and many other reactive functional groups for enzyme immobilization (Leckband and Langer, 1991; López-Gallego et al., 2013; Maeda et al., 2008; Mateo et al., 2007a; Mazi et al., 2006; Tasso et al., 2009; Zhang et al., 2011) The chemical interactions used for surface attachment/adsorption may primarily be divided into three categories, Van der Waals-based adsorption, ionic adsorption, and covalent attachment (Sheldon, 2007).

Van der Waals enzyme adsorption techniques have been successfully used in industry, but because these intermolecular forces are weak in comparison to ionic or covalent bonds, significant leaching of the enzyme from the support occurs over time (Zhao et al., 2006). Ionic adsorption improves retention over Van der Waals interactions, but leaching to a lesser extent is still common (Kirk and Christensen, 2002). Covalent immobilization is best suited for producing the strongest and longest lasting bonds between enzymes and surfaces, however it is the most prone to undesired surface-enzyme interactions resulting in activity loss (Barbosa et al., 2014; Kim et al., 2006; Klibanov, 1979; Mateo et al., 2007b; Mozhaev et al., 1990). Traditionally, all of these techniques are limited in their inability to control the orientation at which the enzyme attaches/adsorbs to the surface to minimize undesired enzyme-surface interactions, maximize enzyme stability, and maximize active-site accessibility (Hernandez and Fernandez-Lafuente,

2011; Mateo et al., 2007b).

The development of technologies to enable site-specific enzyme immobilization at any desired residue on the protein would enable virtually all options. Prior modeling research has predicted that certain attachment sites can minimize undesired enzyme-surface interactions and optimize thermodynamic stability of immobilized proteins and enzymes (Friedel et al., 2007; Talasaz et al., 2006; Wei and Knotts, 2011b; Zhuoyun et al., 2009). Moreover, careful immobilization orientation control can minimize the effects of steric hindrance of the enzyme active site post-immobilization and provide greater understanding of the enzyme-surface interactions.

Previous research demonstrating covalent site-specific immobilization techniques have suffered from significant limitations in potential immobilization locations, such as the N- or C- terminal regions (Smith et al., 2005; Tominaga et al., 2004). Other site-specific immobilization technologies have enabled immobilization at many potential residues, but rely on noncovalent techniques (Kalia et al., 2007; Lim et al., 2014; Seo et al., 2011). To our knowledge, no covalent site-specific immobilization method has been previously demonstrated enabling immobilization at residues throughout the enzyme while only requiring a single substitution or insertion. In this paper, we seek to address the need of a covalent site-specific system enabling immobilization at potential residues throughout the enzyme to prevent enzyme leaching and also analyze the impact of immobilization orientation on enzyme stability.

Here, we report our PRECISE system's (Protein Residue-Explicit Covalent Immobilization for Stability Enhancement) (Smith et al., 2013) effective application for covalent, site-specific immobilization and increased stability of enzymes. This system facilitates easy, non-invasive enzyme recoverability and reusability, testing of enzyme activity at different immobilization sites, and comparisons of enzyme stability when attached at different orientations. These benefits are

accomplished through the use of amber-codon-substitution to enable rationally-directed non-canonical amino acid incorporation for site-specific enzyme immobilization using the covalent, biocompatible, and bioorthogonal Huisgen 1,3-dipolar cycloaddition reaction (Boyce and Bertozzi, 2011; Hong et al., 2010; Smith et al., 2013; Young et al., 2010). The results from these tests indicate that enzyme immobilization orientation plays a significant role in enzyme activity and stability and that meaningful stability enhancements above and beyond that provided by immobilization alone can be found through careful immobilization orientation control.

2. Materials and Methods

2.1 Cloning

A T4 lysozyme variant (Plasmid 18111) with two mutations, C54T and C97A, but equivalent activity and stability to the wild-type lysozyme was acquired from Addgene (Cambridge, MA) (Matsumura and Matthews, 1989). This T4 lysozyme variant simplified cell-free protein synthesis (CFPS) because it eliminated the need to alter the environmental redox potential to promote disulfide bond formation (Matsumura and Matthews, 1989). As an additional benefit, the denaturation pathway of this variant has been well-characterized (Peng and Li, 2008).

For protein purification purposes, a strep-tag (consisting of the eight amino acids Trp-Ser-His-Pro-Gln-Phe-Glu-Lys) was added to the C-terminus of the cysteine-free T4 lysozyme using the Quikchange II mutagenesis protocol (Agilent Technologies, Santa Clara, CA). This T4 lysozyme is hereafter referred to as the "standard" lysozyme. Six sites were selected for modifications to enable non-canonical amino acid incorporation at each site and immobilization at that site. These sites were T21, K35, N53, L91, K135, and K162 and the Quikchange II mutagenesis protocol was used to substitute the amber stop codon at each location (Figure 1A).

2.2 Cell-free Protein Synthesis

The *Escherichia coli* cell-free protein synthesis system is a protein production technology particularly valuable for its scalability (Zawada et al., 2011). Previously researchers have demonstrated equivalent protein production from the 100 µl to the 100 liter scale (Zawada et al., 2011). Here, CFPS reactions for protein production were performed as described previously (Smith et al., 2013). The cell-free extract was prepared as described previously (Shrestha et al., 2014) and was produced from a BL21 Star™ (DE3) *E. coli* strain purchased from Invitrogen (Carlsbad, CA) harboring the pEVOL-pPrF plasmid, a kind gift from Peter Schultz, (Scripps Research Institute). For cell-free reactions for lysozyme variants incorporating non-canonical amino acids, 2 mM p-propargyloxyphenylalanine (pPa) and 3 mg/ml pPa specific *Methanocaldococcus jannaschii* pPa tRNA-synthetase were additionally added (Smith et al., 2013). Post-cell free reaction, lysozyme was purified from the CFPS reaction using Strep-Tactin Superflow columns (IBA Life Sciences, Gottingen, Germany). The lysozyme variants were quantified as described below.

2.3 Protein Yields

The yields for the total and soluble protein were calculated using liquid scintillation as described previously (Smith et al., 2013). Full-length protein production was verified by running sodium dodecyl sulfate polyacrylamide gel electrophoresis, followed by autoradiography as previously reported (Smith et al., 2013). In all reactions where the non-canonical amino acid was not added, all T4 lysozyme proteins were truncated and no full-length protein was observed (Figure 1F). In contrast, where the non-canonical amino acid was added, full-length T4 lysozyme was produced (Figure 1E). Once full-length protein production was verified, soluble proteins were recovered from the supernatant post-centrifugation at 13,000 x g for 15 minutes and purified by strep-

column purification per the manufacturer's specifications (IBA Life Sciences, Goettingen, Germany).

2.4 Enzyme Immobilization on Superparamagnetic Beads

Nonspecific covalent lysozyme immobilization was performed using M-270 Epoxy Dynabeads (Life Technologies, Carlsbad, CA). (Figure 1D). The manufacturer specified protocol was used for immobilization. This immobilization method enables covalent immobilization at all arginines, lysines, and the N-terminus (Figure 1B). 200 µl reactions were used with 300 µM of available epoxy sites and 3 µM lysozyme. The immobilization of the enzyme was verified by liquid scintillation counting of C^{14} leucine-radiolabeled lysozyme.

For site-specific attachment, the Huisgen 1,3-dipolar "click" reaction was used (Figure 1C). Click reaction conditions consisted of 2 mM $CuSO_4$, 10 mM sodium ascorbate, 4 µM THPTA, 300 µM of azide functionalized M-270 Amine Dynabeads as discussed previously, and 3 µM of lysozyme with a total reaction volume of 200 µl (Smith et al., 2013). The reaction was added into a 1.5 ml microcentrifuge tube and rotated end over end for 24 hours at 4ºC. Enzyme immobilization was verified by liquid scintillation counting of C^{14} leucine-radiolabeled lysozyme.

2.5 Purification of Lysozyme Immobilized Dynabeads

Immobilized lysozyme was purified using the following procedure. Microcentrifuge tubes containing reaction mixtures were centrifuged and placed on a Dynaspin Magnet (Life Technologies) for 8 minutes to ensure that all beads were firmly pulled to the microcentrifuge tube sidewalls by the magnet. All reaction reagents except the beads were removed by careful pipetting. Next, careful washing of the beads to remove noncovalently immobilized lysozyme was performed and the buffer was exchanged four times repeating the following procedure. First the beads were resuspended with 100 µl of PBS buffer at 4ºC and vigorous vortexing. After

vortexing, the beads were incubated for 15 minutes at 4ºC. Samples were then returned to the DynaMag Spin Magnet and the supernatant removed by pipetting. After the final washing step was complete, the beads were resuspended and subsequently stored at 4ºC in the Enzchek Lysozyme Assay reaction buffer (Life Technologies, Carlsbad, CA). 1x Enzchek Lysozyme Activity Assay reaction buffer (hereafter referred to as "assay reaction buffer") consists of 0.1 M sodium phosphate, 0.1 M sodium chloride, and 2 mM sodium azide at a pH of 7.5.

Liquid scintillation counting demonstrated that on average 7.7±0.96% of the lysozyme added to the immobilized reaction was conjugated on the superparamagnetic beads. Using surface area data provided by the manufacturer and conservatively assuming that lysozymes would horizontally orient in the most space-saving fashion, it was estimated that at the average coupling efficiency of 7.7%, immobilized lysozymes would cover 53.9% of the surface area of each individual superparamagnetic bead. Thus, higher conjugation efficiencies were likely inhibited by steric hindrances.

2.6 Lysozyme Activity Assay

A standard commercial lysozyme activity assay, the Enzchek Lysozyme Assay Kit (Life Technologies) was used to determine enzyme activities using the following protocol: 2.75 µg of *Micrococcus lysodeikticus* substrate was suspended in assay reaction buffer for a total volume of 50 µl and incubated for 15 minutes at 37ºC. The 50 µl of soluble substrate was added to 50 µl of covalently immobilized Dynabeads suspended in assay reaction buffer or 50 µl of unimmobilized lysozyme suspended in assay reaction buffer. Each 100 µl reaction was added into a Corning Costar 3915 (Corning, NY) black fluorescent 96 well plate. Fluorescein fluorescence released by lysozyme activity was measured per the assay kit instructions for 60 minutes using a Biotek Synergy MX monochromator set to 494 nm excitation and 518 nm emission wavelengths. The

specific activity of each lysozyme was quantified after the 60 minute time point and normalized to the specific activity of the standard unimmobilized and untreated lysozyme. The average concentration of the immobilized and free enzyme concentrations were assessed for activity at 6.1±1.5 μg/ml and 22.1±5.1 μg/ml respectively.

2.7 Freeze Thaw Cycles

50 μl of aliquots of site-specifically bead-immobilized lysozyme, nonspecifically bead-immobilized lysozyme and unimmobilized lysozyme were tested for activity prior to freeze thaw by using the lysozyme activity assay described above. After testing and washing, the lysozyme immobilized beads and a fresh 50 μl aloquot of unimmobilized lysozyme were added to a 96 well plate and carefully sealed to prevent evaporation. The 96 well plate was stored at -80ºC for 20 minutes and then immediately placed at 25ºC for 20 minutes, a change of 105ºC. After the completion of this cycle, the plate was returned to -80ºC for the beginning of the second cycle. Three total freeze thaw cycles were performed. Post-freeze thaw cycles, the lysozyme activity assay was performed to determine change in lysozyme activity after freeze thaw.

2.8 Urea Incubation

50 μl of aliquots of site-specifically bead-immobilized lysozyme, nonspecifically bead-immobilized lysozyme and unimmobilized lysozyme were tested for activity prior to urea denaturation by using the lysozyme activity assay. The assay was slightly modified by the addition of an extra 50 μl of assay reaction buffer (total volume of 150 μl instead of 100 μl). The lysozyme immobilized beads were then washed and stored in microcentrifuge tubes. 50 μl of fresh unimmobilized lysozyme were also added to microcentrifuge tubes. Urea in reaction buffer was added to both sets of lysozyme for a final concentration of 2 M urea and a final volume of 100 μl. Each reaction was then incubated in urea at 37ºC for 30 minutes. After urea incubation,

2.75 µg of *Micrococcus lysodeikticus* substrate solubilized in 50 µl total volume of reaction buffer was added to each urea lysozyme set, creating a total of 150 µl for each reaction. Each reaction was added into a 96 well plate and tested for fluorescence using the same excitation and emission wavelengths described above.

3. Results and Discussion

3.1 Utilizing Non-Canonical Amino Acid Incorporation to Enable the PRECISE System

The PRECISE system enables site-specific, orientation-controlled, covalent immobilization of enzymes onto a chosen carrier or surface. Through the use of rationally directed, site-specific amino acid incorporation, we have previously shown that the model reporter protein GFP's stability significantly improved when subjected to denaturing conditions (Smith et al., 2013). Here, we report for the first time the covalent, site-specific immobilization of enzymes using the PRECISE system. As described in the Material and Methods section, T4 lysozyme was used as a model enzyme. The PRECISE-immobilized T4 lysozyme activity and stability under denaturing conditions is directly compared to the stability of T4 lysozyme immobilized using traditional covalent immobilization techniques. For all immobilizations, superparamagnetic beads were employed as the enzyme carrier due to their nontoxic and biocompatible nature and facilitate non-invasive enzyme recovery (Cao et al., 2012; Dyal et al., 2003; Lei et al., 2007; Yu et al., 2012).

The standard lysozyme, a cysteine-free T4 lysozyme variant from Addgene, was used as a template to create six different lysozyme variants each with a single pPa non-canonical amino acid insertion (Figure 1A). pPa was selected as a non-canonical amino acid enabling a click conjugation reaction (Figure 1C). Variants T21pPa and K35pPa were chosen for their proximity to the activity site with T21pPa directly next to the active site and K35pPa in the same region as the active site. N53pPa, K135pPa, and K162pPa were chosen as sites that had high surface

accessibility and were far from the active site region and for their presence in less structurally important loop regions. L91pPa was selected due to prior work suggesting that it would be an optimal, thermodynamically stable tethering site (Wei and Knotts, 2011a) (Figure 1A).

The nonspecific covalent enzyme immobilization technique targeting all arginines, lysines, and the N-terminus in the enzyme was chosen because it enabled immobilization at any one of many sites distributed relatively equally in the enzyme, near and far from the active site, surface accessible or buried, near or on protein loops, alpha helices, and beta sheets. Given the 26 potential attachment residues (13 arginines, 12 lysines, and the N-terminus), approximately 1 in every 6 residues was a potential immobilization site (Figure 1B, 1D).

Auto-radiograms were performed to ensure that full-length T4 lysozyme variants containing the non-canonical amino acid were produced when the non-canonical amino acid pPa was added (Figure 1E) and that full-length T4 lysozyme was not produced when the non-canonical amino acid was omitted in the CFPS reaction (Figure 1F).

The post-protein purification yield for the standard T4 lysozyme ranged from 0.6 mg to 0.7 mg per 1 ml batch cell-free protein synthesis (CFPS) reaction. CFPS reactions ranging from the 15 µl to the 1 ml scale had similar protein production yields ranging from 0.6 mg to 0.7 mg per 1 ml batch reaction. Because the amber codon substitution system is more complex, the yields for the lysozymes with non-canonical amino acids were lower. The post-purification yield for T21pPa, K35pPa, and L91pPa lysozymes ranged from 0.25 mg to 0.3 mg per 1 ml batch reaction. For N53, K135, and K162, protein yields were typically less than one-third as productive, ranging from 0.04 mg to 0.1 mg per 1 ml batch reaction.

3.2 Activity of the T4 Lysozyme Variants

The insertion of the non-canonical amino acid, pPa, had divergent effects on the activity of each lysozyme variant dependent upon the location of the mutation at each of the six rationally engineered sites (Figure 2). The lysozyme variants immediately next to the active site (T21pPa) and near the active site (K35pPa) suffered the most dramatic decrease in activity, with the lysozyme variant T21pPa retaining less than ten percent of the activity of the standard lysozyme. Given the proximity of the non-canonical amino acid to the active site, these effects were expected and consistent with previous research that report the effect of amino acid mutations near the active site (Greenwald et al., 1999). The three variants that were chosen for their surface accessibility and distance from the active site, N53pPa, K135pPa, and K162pPa, maintained much higher activity, ranging from 70 percent to 85 percent of the activity of the standard lysozyme. The final variant, L91pPa, showed activity in solution that placed it in the middle of the range between the three variants N53pPa, K135pPa, and K162pPa that were further from the active site. These differences in enzyme activity post-unnatural amino acid insertion demonstrate the importance of careful selection of the insertion site.

This data supports avoiding the active site region and choosing surface exposed and flexible areas for non-canonical amino acid incorporation. However, avoiding active sites and choosing surface exposed sites for non-canonical amino acid incorporation becomes difficult in instances where the protein of interest's structure remains unsolved. Given that the Protein Data Bank's approximately 92,000 solved structures remains a small fraction of all known protein sequences, the continued acquisition of data on the effect of non-canonical amino acid incorporation sites on activity and structure as well as the development of better experimentally validated simulation software is needed to realize the full potential of non-canonical amino acid applications.

3.3 Effect of Lysozyme Immobilization on Lysozyme Activity

Due to the consequences of steric effects and steric hindrance in particular, the orientation of the immobilized enzyme can have a significant effect on enzyme activity. To test these effects, lysozyme variants were covalently immobilized on superparamagnetic beads at the non-canonical amino acid site using PRECISE technology (Smith et al., 2013) (Figure 1C). For scaled up production and immobilization the lysozyme variants T21pPa, K35pPa, and L91pPa were specifically chosen because of high protein expression yields in the *E. coli*-based cell-free protein synthesis system and their representation of a location at the active site, a location in the proximity of the active site, and a location away from the active site which is also the best location predicted by simulation (Wei and Knotts, 2011a). The specific activity of each immobilized variant was measured and compared to covalent nonspecifically immobilized standard lysozyme (Figure 3). The activity of standard lysozyme prior to immobilization was used as a conservative control for comparison as it had significantly higher activity than any other lysozyme variant prior to immobilization.

The distinct changes in enzyme activity for each lysozyme variant post-immobilization strongly suggest that immobilization orientation has a significant effect on enzyme activity (Figure 3). As initially predicted, the immobilization next to active site (T21pPa) resulted in a large decrease in specific activity (44% drop). Nonspecifically immobilizing the standard lysozyme also resulted in a similar, large decrease in specific activity in percentage terms (46% drop), although it maintained higher activity in absolute terms than the T21pPa immobilized variant. In contrast, the remaining two site-specifically immobilized variants, L91pPa and K35pPa, exhibited much smaller drops in specific activity (19% and 24% drop respectively). Consequently, L91pPa had the highest absolute activity of all the immobilized lysozyme types post-immobilization (Figure 3). Thus, these results suggest that the advantages of immobilization orientation control in the

demonstrated system can outweigh the costs in enzyme activity due to the incorporation of the non-canonical amino acid.

3.4 Effect of Lysozyme Immobilization Orientation on Lysozyme Activity Retention Post-Freeze Thaw Cycling

Following immobilization, we evaluated the effect of immobilization orientation on activity after subjecting the enzymes to denaturing conditions. For this evaluation immobilized K35pPa, L91pPa and standard lysozyme variants were used. The immobilized T21pPa lysozyme variant was not used due to its very low activity close to background. The immobilized K35pPa variant was included in the stability experiments as it had higher activity than the T21pPa variant and enabled us to examine the effect of near-active site immobilization on post-immobilization lysozyme activity. Given that enzymes are commonly frozen for storage and later thawed for both industrial and research purposes, with the freezing and thawing process producing significant changes in buffer and salt concentrations, which can cause denaturation in the absence of a cryoprotectant, freeze thaw cycles were utilized to assess the role that immobilization orientation plays in promoting or weakening enzyme stability (Pikal-Cleland et al., 2000).

After subjecting the lysozyme variants to three freeze thaw cycles of -80ºC to 25ºC in the absence of a cryoprotectant, the standard lysozyme, K35pPa, and L91pPa variants all suffered a significant decrease in activity, with all enzymes retaining only 20 to 30 percent of their pre-freeze thaw activity (Figure 4). In contrast, all of the immobilized enzymes, specific and non-specific retained significantly greater activity, with far greater activity retention seen with the K35pPa and L91pPa (~70-80% retention) site-specifically attached lysozyme variants compared to nonspecifically immobilized standard lysozyme (42% retention). In absolute terms, immobilized L91pPa was 141% more active than the unimmobilized standard lysozyme post-

freeze thaw and 50% more active than the nonspecifically immobilized standard lysozyme (Figure 4). Thus, although traditional nonspecific enzyme immobilization affords increases in enzyme stability, such stability improvements can be significantly increased through an attachment that enables enzyme immobilization orientation control.

3.5 Effect of Lysozyme Immobilization Orientation on Lysozyme Activity Retention Post-Urea Incubation

The mechanism of urea denaturation is believed to be caused by direct urea-protein interactions and/or by perturbation of solvation environment around the protein by urea, increasing solvation of hydrophobic groups (Hua et al., 2008). Urea denaturation thus acts in a very different denaturation process than freeze thaw cycles, making it another useful tool for evaluating stability.

Similar to the data obtained after freeze thaw denaturation, site-specifically immobilized K35pPa and L91pPa lysozyme variants retained a higher percentage of activity than the nonspecifically immobilized standard lysozyme and all unimmobilized lysozymes. All unimmobilized lysozymes lost the majority of their activity retaining approximately 20 to 40 percent of their pre-urea activity (Figure 5). Similar to the freeze thaw denaturation, both of the site-specifically immobilized lysozyme variants retained more than 70% of their pre-urea incubation activity while the nonspecifically immobilized standard lysozyme lost 67% of its pre-urea activity. On an absolute activity scale, site-specifically immobilized L91pPa lysozyme was more than twice as active as unimmobilized standard lysozyme after urea treatment and was 73% more active than the nonspecifically immobilized standard lysozyme (Figure 5).

4. Conclusion

Here we employ our recently developed PRECISE system to demonstrate for the first time site-

specific covalent immobilization of enzymes at residues throughout the enzyme. Different from prior immobilization techniques, as demonstrated here, the PRECISE system is an entirely covalent immobilization that requires only a single substitution or insertion to facilitate immobilization orientation control (Ewers et al., 2005; Kalia et al., 2007; Lim et al., 2014; Seo et al., 2011; Smith et al., 2005). We have demonstrated that by controlling the immobilization orientation, greater enzyme stability can be realized than nonspecific covalent immobilization, even by 50% and 73%. Improved stability is especially important for developing enzyme biocatalysts capable of long-term reuse and thus enabling economically competitive biocatalyst use in lower margin chemical applications. As a potential industrially relevant carrier, superparamagnetic beads were employed as the immobilized enzyme carriers. These beads provide facile recovery and reuse of the enzymes as was demonstrated during the stability assays. We have also provided preliminary data suggesting that current simulation capabilities may be useful in selecting a good location for enzyme immobilization, with the simulation-predicted L91 site being the most stable location for enzyme immobilization under two different denaturing conditions. Overall, the PRECISE system enables a truly covalent attachment of the enzyme at potential any accessible residue and is an attractive technology to determine the optimal orientation for enzyme immobilization for biocatalysis applications.

Acknowledgments

The authors thank Dr. James Swartz (Stanford University) and Dr. Peter Schultz (Scripps Research Institute) for their generous gifts of the pPaRS and pEVOL-pPrF plasmids. Protein ribbon figures were prepared using the UCSF Chimera software and the respective PDB files (Pettersen et al., 2004). They also acknowledge Dr. Thomas A. Knotts IV and Dr. Wei Shuai for their advice and expertise regarding T4 Lysozyme simulations. This work was supported by

National Science Foundation CBET Division CAREER Award (#1254148), a DARPA Young Faculty Award (#D13AP000037), and a BYU Mentoring Grant.

Figures

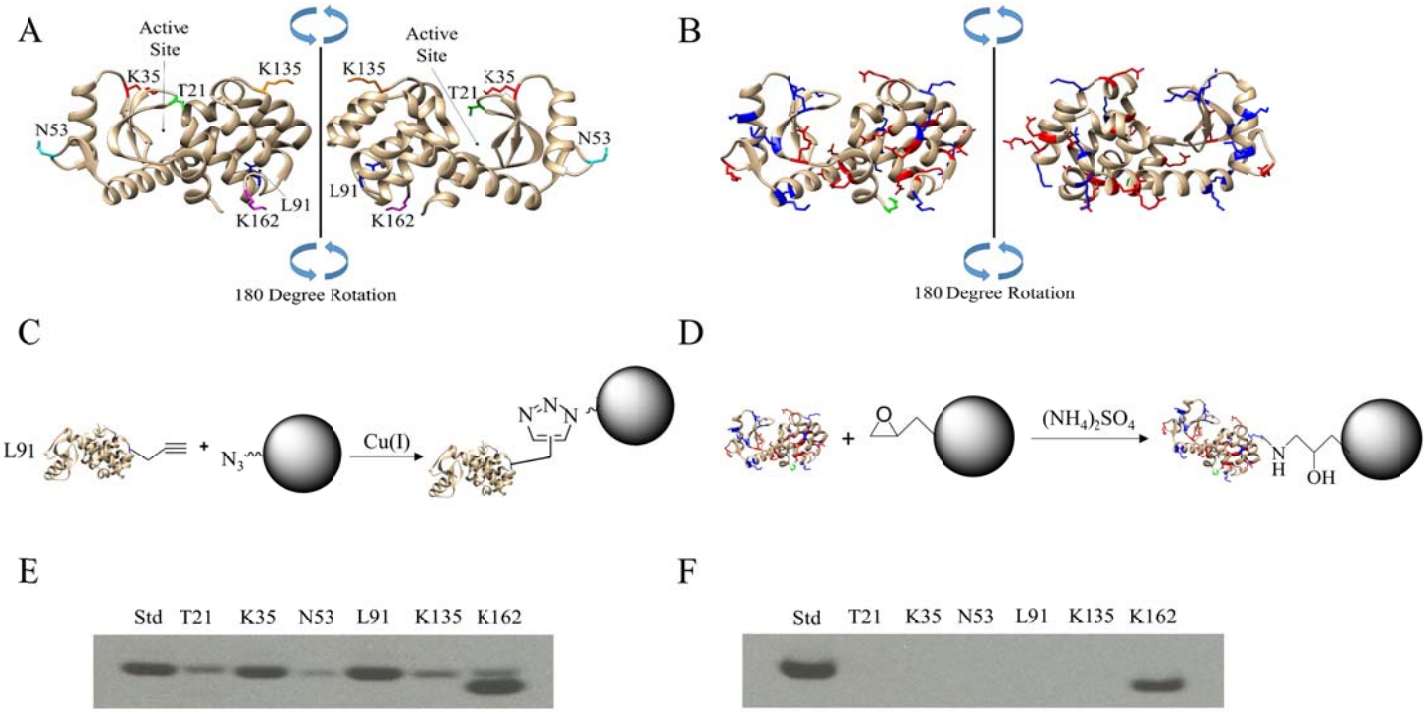

Figure 1. Site-specific vs. Nonspecific Covalent Immobilization. A. Location of six different non-canonical amino acid incorporation sites tested as potential immobilization sites. B. T4 lysozyme structure showing all possible nonspecific immobilization attachment sites at arginines (red), lysines (blue), and the N-terminus (green). C. The PRECISE System attachment scheme utilizing non-canonical amino acid incorporation and the Huisgen 1,3-dipolar cycloaddition ("click" reaction) to site-specifically covalently immobilized enzymes on superparamagnetic beads. D. Nonspecific covalent immobilization scheme using epoxy-functionalized beads treated to bind to reactive amines. E. Autoradiogram demonstrating lysozyme variant protein production when the non-canonical amino acid is added to the cell-free protein synthesis reaction. F. Autoradiogram demonstrating that full-length lysozyme variant production was not detected when the non-canonical amino acid was not added. Note the truncation band for K162 is due to termination of the protein at the amber stop codon, which is only 10 codons from the C-terminus. As all produced proteins were subjected to a strep-tag purification process where such strep-tag was located on the C-terminus of the lysozyme, only full-length proteins were recovered and used for further experiments.

A

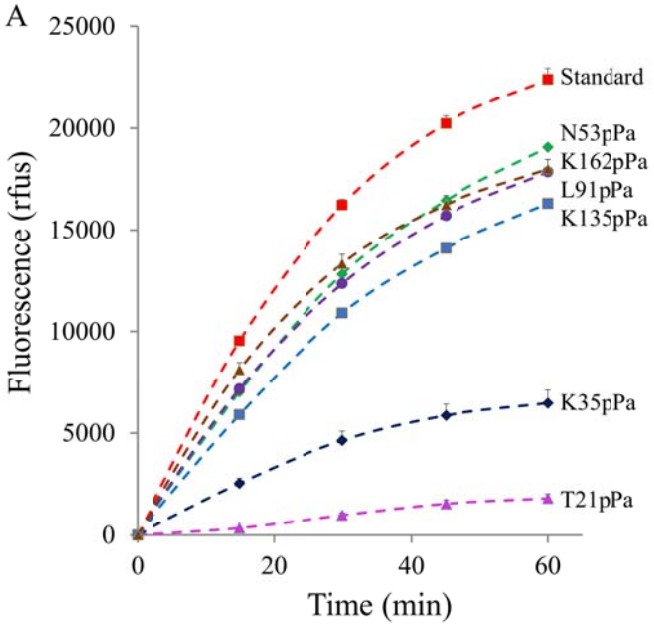

B

Type of Lysozyme	Activity as a % of Standard	Standard Error
Standard	100	N/A
N53pPa	85.2	6.5
K162pPa	80.4	2.2
L91pPa	79.8	2.5
K135pPa	72.8	7.4
K35pPa	28.9	6.2
T21pPa	8.0	6.9

Figure 2. T4 Lysozyme Specific Activity. A. The activity of each lysozyme measured for 60 minutes at 37ºC. The activity shown is normalized for enzyme concentration and thus is a measure of the specific activity of each lysozyme. B. The specific activity of each lysozyme normalized to the specific activity of the standard lysozyme.

A

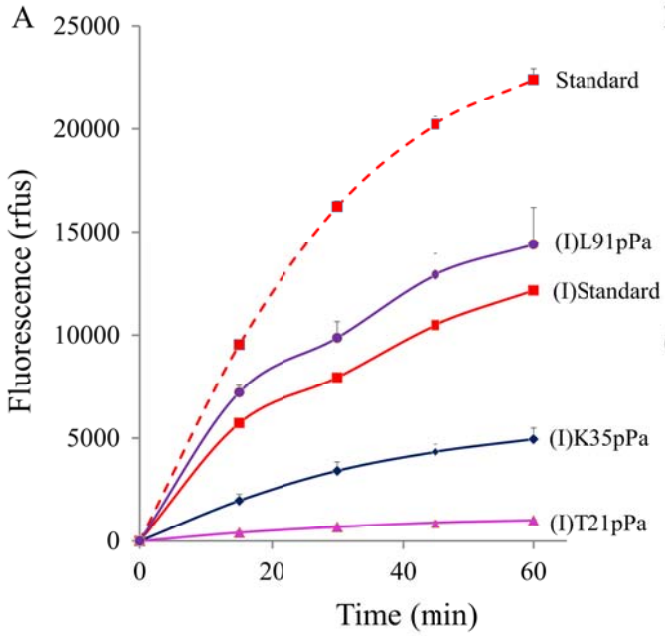

B

Type of Lysozyme	Immobilized	Activity as a % of Standard	Standard Error
Standard		100	N/A
Standard	X	54.3	1.5
L91pPa	X	64.3	7.4
K35pPa	X	22.1	6.7
T21pPa	X	4.5	3.2

C

Type of Lysozyme	Immobilized	% Change in Activity	Standard Error
Standard	X	-45.7	1.5
L91pPa	X	-19.4	7.5
K35pPa	X	-23.4	10.4
T21pPa	X	-43.6	7.7

Figure 3. T4 Lysozyme Specific Activity Post-Immobilization. A. The specific activity of each lysozyme variant measured for 60 minutes at 37ºC. The activity shown is normalized for enzyme concentration and thus is a measure of the specific activity of each lysozyme. The (I) symbol is added to signify each type of lysozyme that is immobilized. B. The specific activity of each immobilized lysozyme normalized to the unimmobilized standard lysozyme. C. Percentage change in lysozyme activity post-immobilization.

1

A

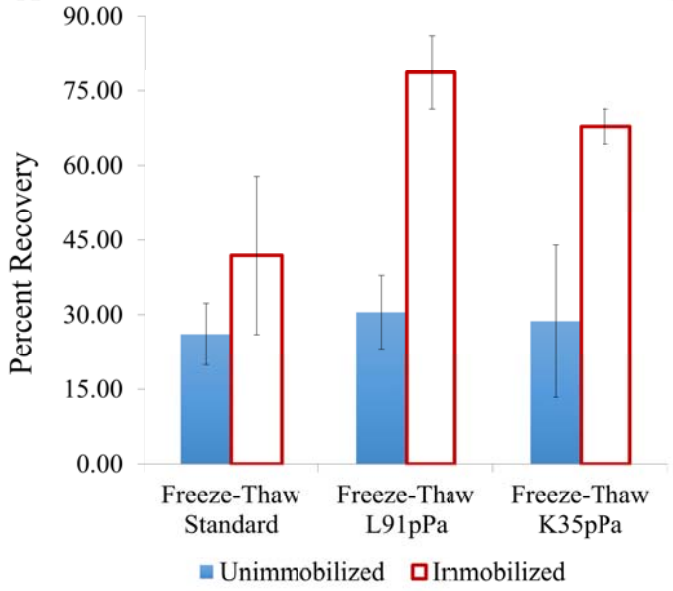

B

Type of Lysozyme	Freeze Thaw Treatment	Immobilized	Activity as a % of Standard	Standard Error
Standard			100	N/A
	X		26.1	6.2
	X	X	41.9	15.9
L91pPa			79.8	2.5
	X		24.3	7.4
	X	X	62.8	7.4
K35pPa			28.9	6.2
	X		8.3	15.3
	X	X	19.6	3.5

2

3 Figure 4. Post-Freeze Thaw Stability. Each lysozyme was subjected to three freeze thaw cycles.
4 Each cycle consisted of 20 minutes at 80°C followed by 20 minutes at 25°C. A. Percent of
5 lysozyme activity retained post-freeze thaw. B. Normalized lysozyme activity standardized to
6 the untreated and unimmobilized standard lysozyme.

7

A

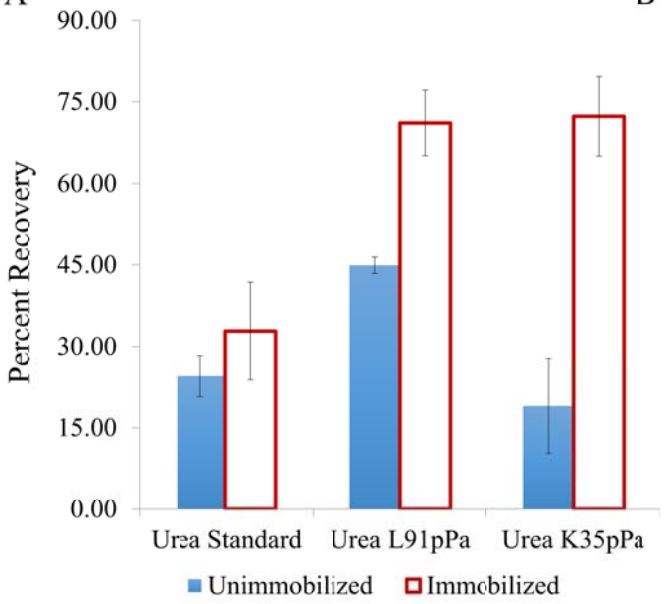

B

Type of Lysozyme	Urea Treated	Immobilized	Activity as a % of Standard	Standard Error
Standard			100	N/A
	X		24.5	3.8
	X	X	32.8	9.0
L91pPa			79.8	2.5
	X		35.8	1.5
	X	X	56.7	6.0
K35pPa			28.9	6.2
	X		5.5	8.7
	X	X	20.9	7.3

Figure 5. Post-Urea Incubation Stability. Each lysozyme was incubated in 2M urea at 37°C for 30 minutes and then assayed for activity. A. Percent of lysozyme activity retained post-urea incubation. B. Normalized lysozyme activity standardized to the untreated and unimmobilized standard lysozyme.

References

Alonso, N., López-Gallego, F., Betancor, L., Hidalgo, A., Mateo, C., Guisan, J.M., Fernandez-Lafuente, R., (2005) Immobilization and stabilization of glutaryl acylase on aminated sepabeads supports by the glutaraldehyde crosslinking method. Journal of Molecular Catalysis B: Enzymatic 35, 57-61.

Anwar, T., Ahmad, B., Younus, H., (2007) Cross-linked stem bromelain: A more stabilized active preparation. Biocatalysis and Biotransformation 25, 453-458.

Barbosa, O., Ortiz, C., Berenguer-Murcia, A., Torres, R., Rodrigues, R.C., Fernandez-Lafuente, R., (2014) Glutaraldehyde in bio-catalysts design: a useful crosslinker and a versatile tool in enzyme immobilization. Rsc Advances 4, 1583-1600.

Bornscheuer, U.T., Huisman, G.W., Kazlauskas, R.J., Lutz, S., Moore, J.C., Robins, K., (2012) Engineering the third wave of biocatalysis. Nature 485, 185-194.

Boyce, M., Bertozzi, C.R., (2011) Bringing chemistry to life. Nature methods 8, 638.

Cao, M., Li, Z., Wang, J., Ge, W., Yue, T., Li, R., Colvin, V.L., Yu, W.W., (2012) Food related applications of magnetic iron oxide nanoparticles: Enzyme immobilization, protein purification, and food analysis. Trends in Food Science & Technology 27, 47-56.

Dyal, A., Loos, K., Noto, M., Chang, S.W., Spagnoli, C., Shafi, K.V.P.M., Ulman, A., Cowman, M., Gross, R.A., (2003) Activity of Candida rugosa Lipase Immobilized on γ-Fe2O3 Magnetic Nanoparticles. Journal of the American Chemical Society 125, 1684-1685.

EPA, (2011) Chemical Manufacturing. U.S. Environmental Protection Agency Sector Profiles.

Ewers, H., Smith, A.E., Sbalzarini, I.F., Lilie, H., Koumoutsakos, P., Helenius, A., (2005) Single-particle tracking of murine polyoma virus-like particles on live cells and artificial membranes. Proc Natl Acad Sci U S A 102, 15110-15115.

Friedel, M., Baumketner, A., Shea, J.-E., (2007) Stability of a protein tethered to a surface. The Journal of Chemical Physics 126, -.

Greenwald, J., Le, V., Butler, S.L., Bushman, F.D., Choe, S., (1999) The Mobility of an HIV-1 Integrase Active Site Loop Is Correlated with Catalytic Activity†,‡. Biochemistry 38, 8892-8898.

Hernandez, K., Fernandez-Lafuente, R., (2011) Control of protein immobilization: Coupling immobilization and site-directed mutagenesis to improve biocatalyst or biosensor performance. Enzyme and Microbial Technology 48, 107-122.

Hong, V., Steinmetz, N.F., Manchester, M., Finn, M.G., (2010) Labeling Live Cells by Copper-Catalyzed Alkyne−Azide Click Chemistry. Bioconjugate Chemistry 21, 1912-1916.

Hua, L., Zhou, R., Thirumalai, D., Berne, B.J., (2008) Urea denaturation by stronger dispersion interactions with proteins than water implies a 2-stage unfolding. Proceedings of the National Academy of Sciences 105, 16928-16933.

Kalia, J., Abbott, N.L., Raines, R.T., (2007) General Method for Site-Specific Protein Immobilization by Staudinger Ligation. Bioconjugate Chemistry 18, 1064-1069.

Kim, J., Grate, J.W., Wang, P., (2006) Nanostructures for enzyme stabilization. Chemical Engineering Science 61, 1017-1026.

Kirk, O., Borchert, T.V., Fuglsang, C.C., (2002) Industrial enzyme applications. Current Opinion in Biotechnology 13, 345-351.

Kirk, O., Christensen, M.W., (2002) Lipases from Candida antarctica: Unique Biocatalysts from a Unique Origin. Organic Process Research & Development 6, 446-451.

Klibanov, A.M., (1979) Enzyme stabilization by immobilization. Anal Biochem 93, 1-25.

Kreiner, M., Parker, M.-C., (2005) Protein-coated Microcrystals for use in Organic Solvents: Application to Oxidoreductases. Biotechnology Letters 27, 1571-1577.

Leckband, D., Langer, R., (1991) An approach for the stable immobilization of proteins. Biotechnology and Bioengineering 37, 227-237.

Lei, Z., Bi, S., Hu, B., Yang, H., (2007) Combined magnetic and chemical covalent immobilization of pectinase on composites membranes improves stability and activity. Food Chemistry 105, 889-896.
Lim, S.I., Mizuta, Y., Takasu, A., Kim, Y.H., Kwon, I., (2014) Site-Specific Bioconjugation of a Murine Dihydrofolate Reductase Enzyme by Copper(I)-Catalyzed Azide-Alkyne Cycloaddition with Retained Activity. PLoS ONE 9, e98403.
López-Gallego, F., Betancor, L., Mateo, C., Hidalgo, A., Alonso-Morales, N., Dellamora-Ortiz, G., Guisán, J.M., Fernández-Lafuente, R., (2005) Enzyme stabilization by glutaraldehyde crosslinking of adsorbed proteins on aminated supports. Journal of Biotechnology 119, 70-75.
López-Gallego, F., Fernandez-Lorente, G., Rocha-Martin, J., Bolivar, J., Mateo, C., Guisan, J., (2013) Stabilization of Enzymes by Multipoint Covalent Immobilization on Supports Activated with Glyoxyl Groups. In: Guisan, J.M. (Ed.), Immobilization of Enzymes and Cells. Humana Press, pp. 59-71.
Maeda, Y., Yoshino, T., Takahashi, M., Ginya, H., Asahina, J., Tajima, H., Matsunaga, T., (2008) Noncovalent Immobilization of Streptavidin on In Vitro- and In Vivo-Biotinylated Bacterial Magnetic Particles. Applied and Environmental Microbiology 74, 5139-5145.
Mateo, C., Grazu, V., Pessela, B.C., Montes, T., Palomo, J.M., Torres, R., Lopez-Gallego, F., Fernandez-Lafuente, R., Guisan, J.M., (2007a) Advances in the design of new epoxy supports for enzyme immobilization-stabilization. Biochem Soc Trans 35, 1593-1601.
Mateo, C., Palomo, J.M., Fernandez-Lorente, G., Guisan, J.M., Fernandez-Lafuente, R., (2007b) Improvement of enzyme activity, stability and selectivity via immobilization techniques. Enzyme and Microbial Technology 40, 1451-1463.
Matsumura, M., Matthews, B.W., (1989) Control of enzyme activity by an engineered disulfide bond. Science 243, 792-794.
Mazi, H., Emregul, E., Rzaev, Z.M., Kibarer, G., (2006) Preparation and properties of invertase immobilized on a poly(maleic anhydride-hexen-1) membrane. J Biomater Sci Polym Ed 17, 821-835.
Milmo, S., (2012) The enzyme makers. Chemistry & Industry 76, 28-31.
Mozhaev, V.V., Melik-nubarov, N.S., Sergeeva, M.V., Šikšnis, V., Martinek, K., (1990) Strategy for Stabilizing Enzymes Part One: Increasing Stability of Enzymes via their Multi-Point Interaction with a Support. Biocatalysis and Biotransformation 3, 179-187.
Peng, Q., Li, H., (2008) Atomic force microscopy reveals parallel mechanical unfolding pathways of T4 lysozyme: Evidence for a kinetic partitioning mechanism. Proceedings of the National Academy of Sciences 105, 1885-1890.
Pettersen, E.F., Goddard, T.D., Huang, C.C., Couch, G.S., Greenblatt, D.M., Meng, E.C., Ferrin, T.E., (2004) UCSF Chimera—A visualization system for exploratory research and analysis. Journal of Computational Chemistry 25, 1605-1612.
Pikal-Cleland, K.A., Rodríguez-Hornedo, N., Amidon, G.L., Carpenter, J.F., (2000) Protein Denaturation during Freezing and Thawing in Phosphate Buffer Systems: Monomeric and Tetrameric β-Galactosidase. Archives of Biochemistry and Biophysics 384, 398-406.
Qiu, G.-M., Zhu, B.-K., Xu, Y.-Y., (2005) α-Amylase immobilized by Fe3O4/poly(styrene-co-maleic anhydride) magnetic composite microspheres: Preparation and characterization. Journal of Applied Polymer Science 95, 328-335.
Rocchietti, S., Ubiali, D., Terreni, M., Albertini, A.M., Fernández-Lafuente, R., Guisán, J.M., Pregnolato, M., (2004) Immobilization and Stabilization of Recombinant Multimeric Uridine and Purine Nucleoside Phosphorylases from Bacillus subtilis. Biomacromolecules 5, 2195-2200.
Seo, M.-H., Han, J., Jin, Z., Lee, D.-W., Park, H.-S., Kim, H.-S., (2011) Controlled and Oriented Immobilization of Protein by Site-Specific Incorporation of Unnatural Amino Acid. Analytical Chemistry 83, 2841-2845.
Sheldon, R.A., (2007) Enzyme Immobilization: The Quest for Optimum Performance. Advanced Synthesis & Catalysis 349, 1289-1307.

Shrestha, P., Smith, M.T., Bundy, B.C., (2014) Cell-free unnatural amino acid incorporation with alternative energy systems and linear expression templates. New Biotechnology 31, 28-34.
Smith, J.J., Conrad, D.W., Cuneo, M.J., Hellinga, H.W., (2005) Orthogonal site-specific protein modification by engineering reversible thiol protection mechanisms. Protein Science 14, 64-73.
Smith, M.T., Wu, J.C., Varner, C.T., Bundy, B.C., (2013) Enhanced protein stability through minimally invasive, direct, covalent, and site-specific immobilization. Biotechnology Progress 29, 247-254.
Talasaz, A.H., Nemat-Gorgani, M., Liu, Y., Ståhl, P., Dutton, R.W., Ronaghi, M., Davis, R.W., (2006) Prediction of protein orientation upon immobilization on biological and nonbiological surfaces. Proceedings of the National Academy of Sciences 103, 14773-14778.
Tasso, M., Cordeiro, A.L., Salchert, K., Werner, C., (2009) Covalent immobilization of Subtilisin A onto thin films of maleic anhydride copolymers. Macromol Biosci 9, 922-929.
Tominaga, J., Kamiya, N., Doi, S., Ichinose, H., Goto, M., (2004) An enzymatic strategy for site-specific immobilization of functional proteins using microbial transglutaminase. Enzyme and Microbial Technology 35, 613-618.
Wang, P., Dai, S., Waezsada, S.D., Tsao, A.Y., Davison, B.H., (2001) Enzyme stabilization by covalent binding in nanoporous sol-gel glass for nonaqueous biocatalysis. Biotechnology and Bioengineering 74, 249-255.
Wang, Y., Caruso, F., (2004) Enzyme encapsulation in nanoporous silica spheres. Chemical Communications, 1528-1529.
Wang, Z.-G., Wan, L.-S., Liu, Z.-M., Huang, X.-J., Xu, Z.-K., (2009) Enzyme immobilization on electrospun polymer nanofibers: An overview. Journal of Molecular Catalysis B: Enzymatic 56, 189-195.
Wei, S., Knotts, T.A., (2011a) Effects of tethering a multistate folding protein to a surface. The Journal of Chemical Physics 134, -.
Wei, S., Knotts, T.A.t., (2011b) Effects of tethering a multistate folding protein to a surface. J Chem Phys 134, 185101.
Young, T.S., Ahmad, I., Yin, J.A., Schultz, P.G., (2010) An Enhanced System for Unnatural Amino Acid Mutagenesis in E. coli. Journal of Molecular Biology 395, 361-374.
Yu, C.-C., Kuo, Y.-Y., Liang, C.-F., Chien, W.-T., Wu, H.-T., Chang, T.-C., Jan, F.-D., Lin, C.-C., (2012) Site-Specific Immobilization of Enzymes on Magnetic Nanoparticles and Their Use in Organic Synthesis. Bioconjugate Chemistry 23, 714-724.
Zawada, J.F., Yin, G., Steiner, A.R., Yang, J., Naresh, A., Roy, S.M., Gold, D.S., Heinsohn, H.G., Murray, C.J., (2011) Microscale to manufacturing scale-up of cell-free cytokine production—a new approach for shortening protein production development timelines. Biotechnology and Bioengineering 108, 1570-1578.
Zhang, Y., Tang, Z., Wang, J., Wu, H., Lin, C.-T., Lin, Y., (2011) Apoferritin nanoparticle: a novel and biocompatible carrier for enzyme immobilization with enhanced activity and stability. Journal of Materials Chemistry 21, 17468-17475.
Zhao, X.S., Bao, X.Y., Guo, W., Lee, F.Y., (2006) Immobilizing catalysts on porous materials. Materials Today 9, 32-39.
Zhuoyun, Z., Andrew, I.J., Patricia, S., Joan-Emma, S., (2009) The effect of surface tethering on the folding of the src-SH3 protein domain. Physical Biology 6, 015004.